Proceedings of ICRC 2001: 3706 © Copernicus Gesellschaft 2001

ICRC 2001

Effects of the termination shock on 16 MeV electron modulation

S. E. S. Ferreira[1], **M. S. Potgieter**[1], **and C. Lopate**[2]

[1]Unit for Space Physics, Potchefstroom University for CHE, 2520 Potchefstroom, South Africa
[2]Enrico Fermi Institute, University of Chicago, Chicago IL 60637, USA

Abstract. The effects of the heliospheric termination shock on electron modulation are illustrated using a shock-drift-modulation model. In particular the model computations are compared to ~16 MeV observations from Pioneer 10. The effects of different shock radii, heliospheric boundary positions and local interstellar spectra on the model computations are illustrated and discussed.

1. Introduction

The study of the modulation of cosmic ray electrons in the heliosphere is an important tool in understanding various aspects of heliospheric modulation. Modulated electron intensities in the lower-MeV range give a direct indication of the average parallel and perpendicular mean free paths in contrast to protons that experience adiabatic energy changes below ~300 MeV (e.g., Haasbroek et al. 1997). Gradient and curvature drifts become less important for electron modulation at lower energies, with almost no effect below 100 MeV (e.g., Ferreira et al. 2000). The Pioneer 10 radial-intensity-profiles for ~16 MeV electrons (Lopate 1991; Lopate 2001) indicate almost no radial gradients out to ~70 AU, which put serious constraints on the diffusion tensor. New computations of the local interstellar spectra (LIS) (e.g., Strong et al., 2000; Langner et al., 2001), indicate that the electron LIS may be considerably lower at energies below ~100 MeV than previously assumed (e.g., Strong et al. 1994). For this work, the effect of these different LIS scenarios and their subsequent modulation in the heliosphere are studied using a shock-drift-modulation model. Satisfying the constraints imposed on the diffusion tensor by the Pioneer 10 electron data in the outer heliosphere, the effects of the location of the heliospheric termination shock (TS) and the heliospheric boundary on electron modulation are also illustrated

2. Modulation model and parameters

The model is based on the numerical solution of Parker's (1965) transport equation (TPE) :

$$\frac{\partial f}{\partial t} = -(\boldsymbol{V} + \langle \boldsymbol{v}_{\mathbf{D}} \rangle) \cdot \nabla f + \nabla \cdot (\boldsymbol{K}_s \cdot \nabla f) + \frac{1}{3}(\nabla \cdot \boldsymbol{V}) \frac{\partial f}{\partial \ln R} + Q, \quad (1)$$

where f ($\boldsymbol{r}$,P,t) is the cosmic ray distribution function; P is rigidity, $\boldsymbol{r}$ is position, and t is time. Terms on the right-hand side represent convection, gradient and curvature drifts, diffusion, adiabatic energy changes and the source function, respectively, with $\boldsymbol{V}$ the solar wind velocity. The symmetric tensor $\boldsymbol{K}_s$ consists of a parallel diffusion coefficient $K_{\parallel}$ and two perpendicular diffusion coefficients, namely $K_{\perp r}$ the perpendicular diffusion coefficient in the radial direction and $K_{\perp \theta}$ the perpendicular diffusion coefficient in the polar direction. The anti-symmetric element K_A describes gradient and curvature drifts, with averaged drift velocity $\boldsymbol{v}_{\mathrm{D}}$, in the large scale heliospheric magnetic field (HMF). The diffusion coefficients and source function Q for Jovian electrons are given by Ferreira et al. SH3.1. The HMF was modified according to Jokipii and Kóta (1989) which is qualitatively supported by Ulysses measurements (Balogh et al., 1995). The TPE was solved time-dependently, using the basic two dimensional TS code developed by le Roux et al. (1996), and expanded by Haasbroek (1997). The current sheet "tilt angle" was fixed at α = 15°. The outer modulation boundary radius, r_b, was assumed at 120 AU, but the effects of r_b = 130 and 140 AU on computations are also illustrated. A TS with a compression ratio of $3.2 < s < 4.0$, and scale length of L = 1.2 AU was assumed at r_s = 90 AU. However, the effects of r_s = 80 and 100 AU on model computations are also illustrated. The solar wind speed V was assumed to change from 400 km.s^{-1} in the equatorial plane ($\theta = 90^{o}$) to a maximum of 800 km.s^{-1} when $\theta < 60^{o}$. At the shock, V decreases in the equatorial plane from the upstream value of V_1 = 400 km.s^{-1} according to the relationship given by le Roux et al. (1996):

$$V(r) = \frac{V_1(s+1)}{2s} - \frac{V_1(s-1)}{2s} \tanh\left(\frac{r - r_s}{L}\right) \quad (2)$$

This translates into a decrease of a factor ~4 in V for the region between the TS and the outer boundary. This decrease is also simulated in the diffusion coefficients.

Correspondence to: S. Ferreira (fsksesf@puknet.puk.ac.za)

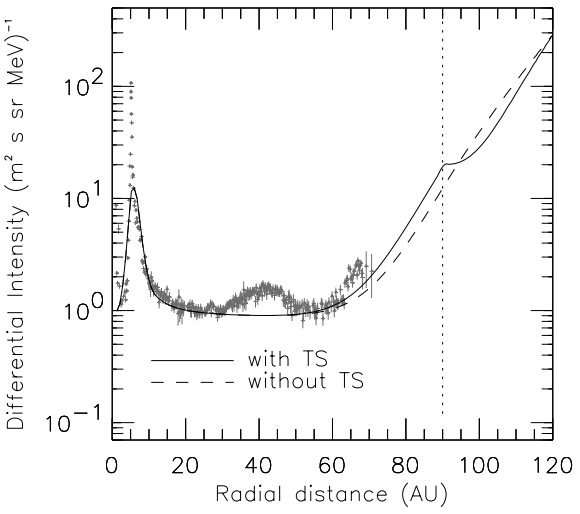

Fig. 1. Computed radial profiles of 16 MeV electron intensities with an outer boundary at r_b = 120 AU. The solid line corresponds to a solution with the TS assumed at r_s = 90 AU, and the dashed line to a solution without the TS. In comparison the ~16 MeV Pioneer 10 (Lopate 1991; Lopate 2001) electron data are shown.

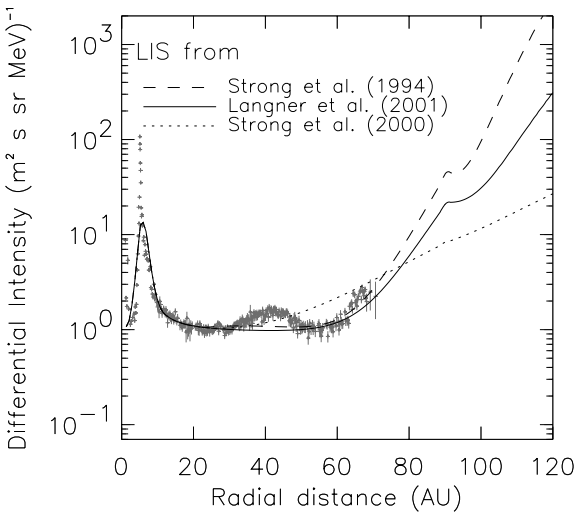

Fig. 2. Same as in Fig. 1., but now three computed scenarios are shown corresponding to three different published LIS's. The LIS of Strong et al. (1994) is shown as the dashed line, the LIS from Langner et al. (2001) as the solid line, and the third LIS, the lowest LIS from Strong et al. (2000), as the dotted line.

3. Results and discussion

Shock vs. Non-shock: Figure 1 shows the radial profile of computed 16 MeV electron intensities with an outer boundary at r_b = 120 AU, where the LIS of Langner et al. (2000) is assumed. In comparison the observed ~16 MeV Pioneer 10 observations (Lopate 1991; Lopate 2001) are shown. Two different model scenarios are shown, the first (solid line) with the inclusion of the TS, and the second (dotted line) without the TS. The Jovian magnetosphere which is a strong source of electrons with energies up to ~30 MeV (e.g., McDonald et al., 1972; Simpson et al., 1974) is clearly visible for r < 10 AU. Apart from the Jovian encounter there is no radial dependence evident in the computed intensities up to ~60 AU, as indicated by the Pioneer 10 data, except for the factor of two increase due to solar activity. For r > 60 AU, the computed radial dependence increases sharply until the value of the LIS is reached at 120 AU.

Compared to the scenario without the TS, the effect of the inclusion of the TS is visible around r_s = 90 AU. The radial gradient increases upstream of the shock because the shock serves as a source of electrons which have been accelerated from lower energies up to 16 MeV. Beyond the shock, the radial gradient decreases because the diffusion coefficients decrease by a factor ~4 in this region. The effect of the TS results in a factor of maximum ~1.3 difference with respect to the non-shock solution implying that the effect of the TS at these low energies is not significant.

Effect of different LIS's: Figure 2 shows the effect of different LIS scenarios on model computations. Three solutions are shown corresponding to three different published LIS's. The parameters used to compute compatibility with the Pioneer 10 data for the different LIS scenarios are given in Ferreira et al., SH3.1.

For the lowest LIS (Strong et al., 2000), the effect of the TS on model computations is barely visible. As the value of the LIS increases at the modulation boundary, the effect of the TS becomes more pronounced. This is because there is more low-energy electrons available to be accelerated at the TS. In order to get compatibility with the observations for r > 10 AU, the diffusion coefficients had to be made smaller for the highest LIS compared to the lowest LIS (see Ferreira et al. SH3.1) which also leads to more effective acceleration of electrons at the TS.

Changing the TS radius: The effects of different positions of the TS on model computations are shown in Fig. 3. Three scenarios are shown corresponding to three different values of r_s, with r_b = 120 AU.

The effect of the shock is evident in all three scenarios. For a TS at r_s = 80 AU, the effect of the shock on the radial

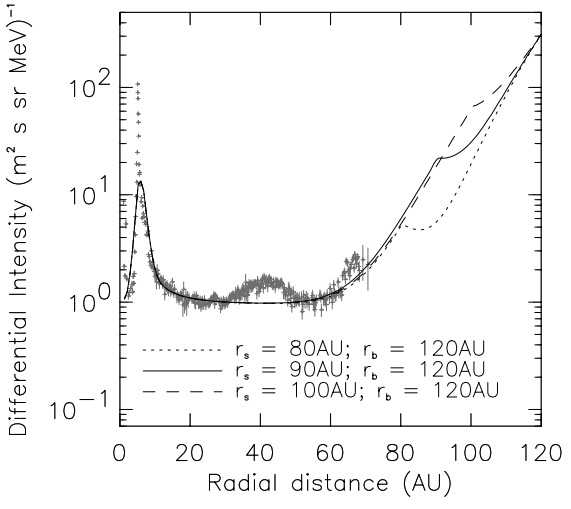

Fig. 3. Same as in Fig. 2, but now for three scenarios corresponding to three different values of r_s. The dotted line corresponds to r_s = 80 AU, the solid line to r_s = 90 AU and the dashed line to r_s = 100 AU.

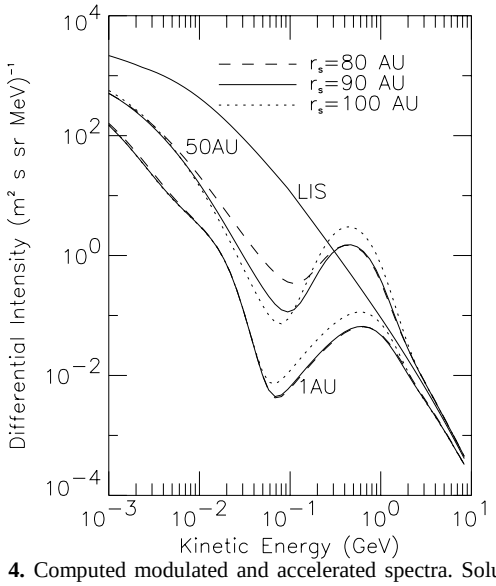

Fig. 4. Computed modulated and accelerated spectra. Solutions are shown at 1 AU and 50 AU in the equaotrial plane. The dotted line corresponds to a TS at r_s = 80 AU, the solid line at 90 AU and the dashed line at 100 AU.

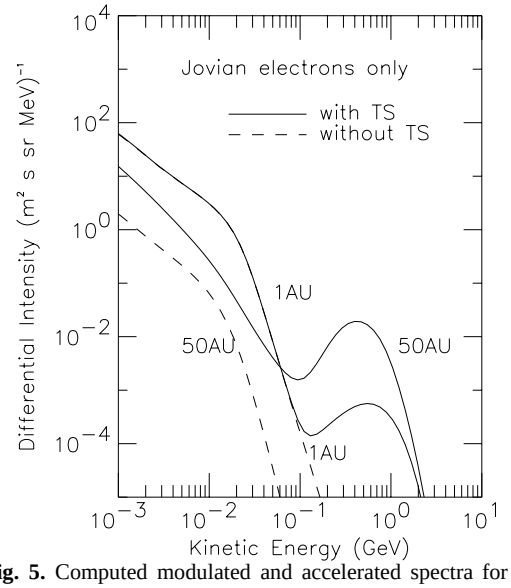

Fig. 5. Computed modulated and accelerated spectra for the Jovian electrons only. Solutions are shown at 1 AU and 50 AU in the equaotrial plane. The solid line with a TS at r_s = 90 AU, but the dashed line without a TS in the model.

gradients upstream and downstream of the shock is significantly larger than the other two scenarios. Although the shock should be more effective for larger shock radii, the radial diffusion coefficient (Ferreira et al., SH3.1), is also becomes larger, leading to a smaller overall effect at this energy for the more distant shocks.

Shocked spectra: The effect of the TS on electron spectra is shown in Fig. 4. It shows the effect of the TS on electron spectra (Jovian and galactic) at 1 AU and 50 AU in the equatorial plane. Three solution scenarios corresponding to three different positions of the TS are shown. The effect is evidently more pronounced at the energies between ~200 MeV and ~2 GeV, with the low-energy electrons being accelerated to these higher energies. For the larger radial distances (here 50 AU) and for E > ~200 MeV, the electrons are accelerated to intensities above the LIS for all values of r_s. As r_s was increased the intensities decreased for E < ~100 MeV, but increased for E > ~100 MeV. This is because the low-energy electrons are more effectively accelerated due to a larger shock radius. At 1 AU there was no effect of the TS on the spectra for E < 50-100 MeV, because of the domination of the Jovian source at these energies, but above this energy, the intensities do increase when r_s increased.

Compared to the galactic electrons the re-acceleration of the Jovian electrons is negligible (see also e.g., Haasbroek et al., 1997) as illustrated in Fig. 5 where modulated (dashed line) only, and modulated-accelerated (solid line) Jovian spectra are shown at 1 AU and 50 AU in the equatorial plane . The Jovian source is present at 5 AU. At 1 AU and 50 AU the effect of the TS on Jovian electrons is however clearly visible for E > 100 MeV when compared to the solution without a TS. However, compared to the re-accelerated galactic electron intensities as shown in Fig. 4, the re-accelerated Jovian electron intensities are negligible at 1 AU and at 50 AU.

It follows from Fig. 4 that at Earth and for $E \geq 100$ MeV the intensity due to r_s = 100 AU is much higher than for the other r_s scenarios. However, the effect of r_s on model solutions is not linear. Figure 6 shows the 1 GeV electron intensity at Earth as a function of r_s. Also shown are the computed intensity value without a TS in the model.

Figure 6 shows that the TS results in a factor of ~3 more electrons at Earth at 1 GeV due to the acceleration of the low-energy electrons. This is in good agreement of ~2.8 found by Haasbroek (1997) and Haasbroek et al. (1997) using a similar model but different diffusion coefficients. As r_s increases, the intensities initially increases slowly and then more steeply up to r_s = 100 AU. Here the intensities are a factor of ~5 higher than the non-shock solution. Although the effect of this parameter is not as pronounced at 16 MeV which is shown in Figure 3, the effect at 1 GeV is much larger.

Changing the outer boundary radius: The effect of

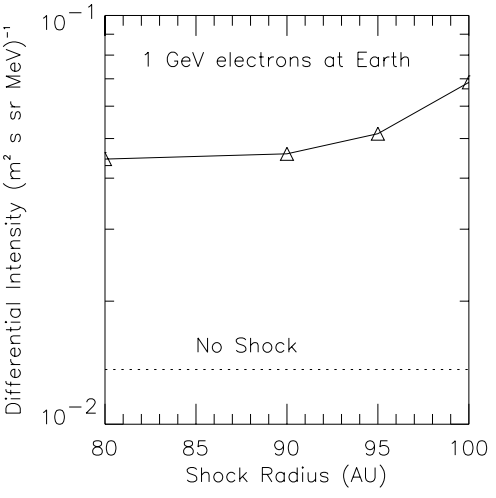

Fig. 6. Computed intensities at 1 GeV as a function of the shock radius r_s, with the modulation boundary at 120 AU. The

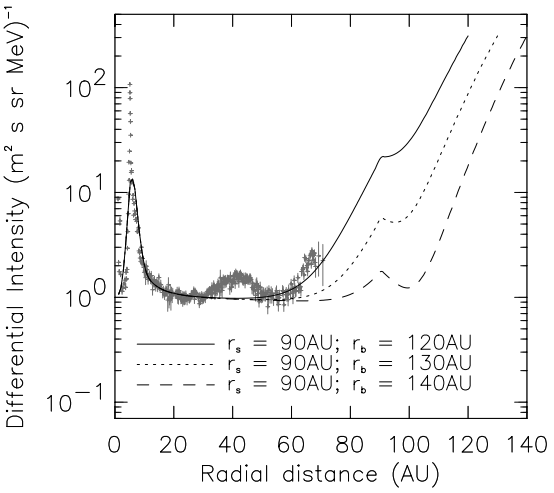

Fig. 7. Same as in Fig.2, except that three scenarios are shown corresponding to three different values of r_b in the model. The solid line corresponds to r_b = 120 AU, the dotted line to r_b = 130 AU and the dashed line to r = 140 AU.

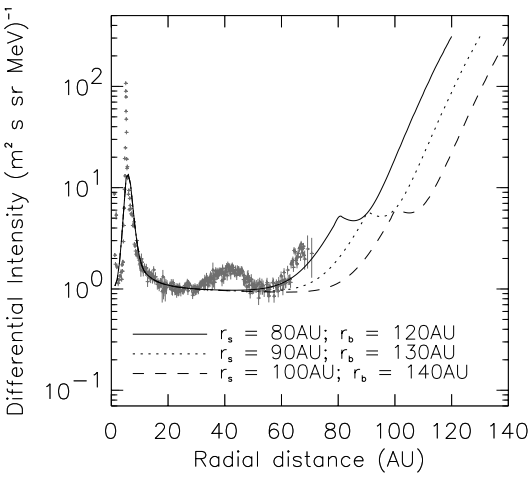

Fig. 8. Same as in Fig. 2, except that three scenarios are shown corresponding to three different values of r_s. The distance between the outer boundary and the TS was assumed fixed at 40 AU. Solid line corresponds to r_s = 80 AU (r_b = 120 AU), dotted line to r_s = 90 AU (r_b = 130 AU), and the dashed line to r_s = 100 AU (r_b = 140 AU).

different positions of the heliospheric boundary on model computations are illustrated in Fig. 7. The computed radial profiles are shown for three different values of r_b. For all three scenarios r_s = 90 AU. Figure 7 shows that this parameter is much more important at 16 MeV than r_s which is shown in Fig. 3. For an increasing r_b the radial gradient keeps constant up to larger distances, but then increases significantly up to the outer boundary. The effect of the TS also becomes more pronounced. Unfortunately, data up to only ~70 AU was measured by Pioneer 10. Therefore, for this model both the r_b = 120 AU and r_b = 130 AU scenarios seem reasonable when compared with the observations.

Changing the shock and boundary radii: In Fig. 8 the distance between the shock and the heliospheric boundary was set to be fixed at 40 AU. The position of the TS was changed from 80 AU to 100AU with the modulation boundary always 40 AU further away. Figures 3 and 7 illustrated that when the position of the TS and the boundary was changed individually, the computed radial dependence changed for the different solutions. Keeping the distance between the shock and the boundary constant, Fig. 8 shows that the radial dependence of the computed intensities remains simialr for the three different computed scenarios. The only difference is that the solutions for an increasing r_s have a constant radial dependence up to larger distances, away from the Sun. The effect of the TS is also unaltered.

3. Conclusions

A two-dimensional numerical shock-drift model, including a Jovian electron source, was used to study the effects of the TS on electron spectra and radial profiles. In particular, the model were compared to observed ~16 MeV Pioneer 10 data. The following is concluded:

1. The effect of the TS on model computations is not as pronounced at E = 16 MeV than for e.g., E > 100 MeV.
2. The effect of the TS is more pronounced the higher the LIS is made at the assumed modulation boundary.
3. The TS results in a factor of ~3 more electrons at 1 GeV at Earth than a non-TS when r_s = 90 AU. As r_s increases, this factor also increases. However, the effect of changing the TS radius on 1 GeV electron intensities is not linear.
4. If the distance between the shock and boundary is kept constant at 40 AU, the radial dependence of the intensities, and the effect of the TS remain similar regardless of the position of the TS.
5. The effect of changing the modulation boundary radius has a larger effect on model computations than changing the shock radius.

Acknowledgements. We thank the S.A. NRF and NASA (Grants NAG 5-6472 and NAG 5-8032) for financial support and H. Fichtner and B. Heber for discussions.

References

Balogh, A., Smith E. J., Tsurutani, B. J., Southwood, D. J., et al., *Science, 268*, 1007, 1995.
Haasbroek, L. J., Ph.D thesis, Potchefstroom University, 1997.
Haasbroek, L. J., Potgieter, M. S., and le Roux, J. A., *Adv. Space Res., 19*, 953, 1997.
Jokipii, J. R. and Kóta, J., *Geophys. Res. Lett., 16*, 1, 1989
le Roux, J. A., Potgieter, M. S., and Ptuskin, V. S., *J. Geophys. Res., 101*, 4791, 1996.
Lopate, C., *Proc. 23rd ICRC, 3*, 415, 1991.
Lopate, C., *J. Geophys. Res.*, submitted, 2001.
Langner, U. W., de Jager, O. C., and Potgieter, M. S., *Adv. Space. Res.*, in press 2001
McDonald, F. B., Cline, T. L., and Simnett, J. G., *J. Geophys. Res., 77*, 2213, 1972.
Parker, E. N., *Planet. Space Sci., 13*, 9, 1965.
Simpson, J. A., Hamilton, D., Lentz, G., McKibben, R. B., et al., *Science, 183*, 306, 1974.
Strong, A. W., Bennett, K., Bloemen, H., Diehl, R., et al., *Astron. Astrophys., 292*, 82, 1994.
Strong, A. W., Moskalenko, I. V., and Reimer, O., *Astrophys. J.*, 537, 763, 2000.